Membrane Binding and Self-Association of α-Synucleins†

Vijaya Narayanan and Suzanne Scarlata*

Department of Physiology & Biophysics, State University of New York at Stony Brook, Stony Brook, New York 11794-8661

Received December 28, 2000; Revised Manuscript Received March 20, 2001

ABSTRACT: Although its function is unknown, α-synuclein is widely distributed in neural tissue and is the major component in the pathological aggregates found in patients with Parkinson's disease, Alzheimer's disease, Down's syndrome, and multiple system atrophy. In this report, we have quantified the binding α-synucleins to lipid membranes. In contrast to previous studies, we find, using real time equilibrium fluorescence methods, that α-synuclein binds strongly to large, unilamellar vesicles with either anionic or zwitterionic headgroups. Membrane binding is also strong for *β*-synuclein, phosphorylated α-synuclein, and a synuclein mutant that is associated with familial Parkinson's disease. In solution at less than 400 nM, synuclein has a tendency to undergo concentration-dependent oligomerization as determined by changes in intrinsic fluorescence and fluorescence resonance energy transfer. Above this concentration, the protein begins to aggregate into structures visible by light scattering. Although membrane binding does not affect the secondary structure of α-synuclein, it greatly inhibits the ability of this protein to self-associate. Taken together, our results indicate that pathological conditions may be associated with a disruption in synuclein−membrane interactions.

α-Synuclein is the major component of lesions associated with several neurological diseases including Parkinson's disease, multiple system atrophy, Hallervorden−Spatz disease (*1*), Lewy body variant of Alzheimer's disease, and dementia with Lewy bodies (for a review, see *2*). These diseases are typified by cellular inclusions consisting mainly of α-synuclein aggregates which form structures such as Lewy bodies in Parkinson's disease, amyloid plaques in Alzheimer's disease, glial cytoplasmic inclusions, and aggregates in presynaptic terminals in multiple system atrophy (MSA) and amyotrophic lateral sclerosis (ALS). Mutants of α-synuclein have been identified in some types of familial Parkinson's disease (*3, 4*). Interestingly, the closely related *γ*-synuclein is overexpressed in breast carcinoma and ovarian cancer and is correlated with disease progression (*5*). Recent studies have directly linked the formation of these fibrils to oxidation and nitration of synuclein tyrosines (*6, 7*).

There are three types of synucleins (α, *β*, and *γ*) that are highly conserved between species, suggesting that they serve some critical function (*8*). However, their function is unclear. Recent work indicates that α-synuclein plays a role in neural plasticity. In support of this idea, α-synuclein appears concentrated around nerve cell bodies in early development, but this localization changes as the development of the central nervous system progresses. On the cellular level, it has been shown that α- and *β*-synucleins inhibit phospholipase D2, which is an enzyme involved in vesicular trafficking (*9*). Synuclein expression also correlates with localization of proteins in the phosphoinositol second messenger system. This finding, coupled with the observation that synucleins will bind to small, unilamellar vesicles (*10*), has implicated the involvement of these proteins in the release and recycling of synaptic vesicles in response to signals transduced through the inositol pathway. To add further complexity, phosphorylated α-synucleins have been detected, but how phosphorylation may change the properties of the protein is unknown (*11, 12*).

Since the diseases associated with α-synuclein appear to involve aggregation and fibril formation, in vitro studies of synuclein association have been conducted. In solution at high concentrations, α-synuclein will form fibrils that resemble Lewy bodies (*13*). Fibril formation occurs by an initial nucleation event, followed by a lag period and a growth phase (*14*). In a study comparing fibril formation of native and mutant synucleins, it was found that all the proteins began to nucleate at the same concentration, but that the rate of fibril growth is much higher in the mutant than in the native protein (*14*). A recent study has identified a stretch of 12 residues in the hydrophobic domain of the protein as responsible for fibril formation (*15*).

By linear sequence, synucleins have 11-residue repeated domains in a pattern similar to that found in the lipid-association proteins, apolipoproteins. This similarity has sparked a series of studies to determine the ability of synuclein to bind to membranes. Davidson et al. (*10*) incubated α-synuclein with highly curved small, unilamellar vesicles for 1−2 h and, after using chromatography to separate bound and unbound lipid, found that α-synuclein would specifically bind to these tightly curved vesicles only if the surface charge of the membranes was negative. Subsequent studies, also using prolonged incubation and mechanical separation methods, indicated that phosphatidylethanolamine lipids promoted binding (*16*). Since the C-terminal region of synuclein has a high percentage of anionic residues, and the N-terminus is apolipoprotein-like, membrane binding was proposed and later confirmed to be

† This work was supported by a seed grant from SUNY-USB BNL collaborative efforts and NIHGM53132.

* Address correspondence to this author. E-mail: suzanne@dualphy.pnb.sunysb.edu; Phone: 631-444-3071; Fax: 631-444-3432.

10.1021/bi002952n CCC: $20.00
Published on Web 07/28/2001

through the N-terminus. Concurrent with membrane association was a shift in the CD spectra from an initial random coil conformation to a helical conformation. Neutralizing the membrane charge or reducing the curvature of the vesicles eliminated the observed binding, supporting the idea that these proteins play a role in vesicle function at the presynaptic terminal. At very high protein concentrations, α-synuclein will disrupt planar lipid bilayers to form aggregates and fibrils (*13*), indicating that membrane association may play a role in the pathophysiology of these neurodegenerative diseases.

In this study, we have applied real time equilibrium methods to quantitatively determine the affinity of synucleins to large, unilamellar vesicles. Unlike previous reports, we find that synuclein has a strong affinity for both negatively charged and electrically neutral lipid membranes. Initial binding to membranes does not affect secondary structure. The relative affinities for these two types of membranes are similar for wild-type α-synuclein, *β*-synuclein, phosphorylated synuclein, and the A53T mutant. In our experiments, we have also found that in solution, α-synuclein has an inherent property whereby even at very low (nanomolar) concentrations, the monomers reversibly associate in a pattern that can be correlated to the formation of early, premature fibrils. Interestingly, our results indicate that membrane binding reduces this early level of oligomerization, leading to the hypothesis that a disruption in lipid interactions may play a role in the pathology of these neurodegenerative diseases.

MATERIALS AND METHODS

Protein Expression and Purification. E. coli expressing α- and *β*-synuclein, and A53T were kindly provided by Andrew Morris (Department of Cell Biology, University of North Carolina). The purification procedure that we followed was similar to that described by Jenco et al. (*9*). One liter cultures of bacteria were grown to an optical density of about 1 at 37 °C. The cells were induced with 0.4 mM IPTG for 1 h at 37 °C. Cell paste obtained from spinning the cultures was stored at −80 °C until further use. For purification, cells were resuspended in TED buffer (20 mM Tris-HCl, pH 8.0, 1 mM EDTA, 1 mM DTT) and disrupted by 5−6 sonication pulses at 13 W at 10−15 s/pulse. Thereafter, cells were centrifuged using a Ti45 rotor at 35 000 rpm for 1 h. The supernatant was placed in a 65 °C water bath for 40 min. A clear supernatant was recovered after centrifugation for 30 min at 35 000 rpm, run over a 15Q column, and eluted with TED buffer containing 0−400 mM NaCl. Fifty 1 mL fractions were collected, and usually synuclein was present in fractions 42−48. These fractions were pooled and diluted into HED buffer (20 mM Hepes, pH 7.4, 1 mM EDTA, 1 mM DTT). Final purification was done over a heparin−Sepharose column using elution with 0−500 mM NaCl. Phosphorylated proteins were a gift from Jeffrey Benovic (Thomas Jefferson University) and were prepared as described by those authors (*12*). Protein concentrations were measured by the BioRad dye binding assay.

SDS−PAGE and Western Blotting. Protein purification was monitored on 12% SDS−polyacrylamide gels where synucleins, which run close to 19 kDa, were visualized by Coomassie Blue staining. Proteins blotted on nitrocellulose were probed using PER1 antibody (*9*) and visualized using the alkaline phosphatase assay. In some instances, the protein bands were also visualized using a silver staining procedure. Irreversibly aggregated protein ran at a high molecular mass of about 66 kDa or above (Figure 1).

Vesicle Preparation. POPS (1,2-palmitoyloleoylphosphatidylserine) or POPC (1,2-palmitoyloleoylphosphatidylcholine), solubilized in chloroform, was dried to a thin film in small round-bottomed flasks using a rotary evaporator. Dried lipid was suspended in 20 mM Hepes/150 mM NaCl buffer to give a concentration of 2 mM, layered with nitrogen, and taken through 10 alternating freeze−thaw cycles using liquid nitrogen and a 37 °C water bath. Vesicles were freshly extruded through a 100 nm pore filter before every experiment to produce large unilamellar vesicles (LUVs).

Fluorescence Experiments. Fluorescence measurements were made using an ISS fluorometer (I.S.S., Inc., Champaign, IL) with samples contained in microcuvettes with a path length of 3 mm. Three types of fluorescence assays were done in this series of experiments. They are briefly outlined below.

(A) Intrinsic Fluorescence. We monitored lipid binding or synuclein self-assembly by changes in the fluorescence emanating from the four synuclein tyrosine side chains. Emission spectra were recorded from 300 to 400 nm after exciting at 278 nm, and were monitored as unlabeled protein or lipid was added. In this latter case, corrections were made for background vesicle scatter.

(B) Laurdan Fluorescence. Lipid bilayers were fluorescently labeled with Laurdan by adding 0.2 mol % Laurdan from a concentrated stock and sonicating at low energy for 3−5 min. These vesicles were then titrated into a 200−500 nM synuclein solution, and the emission from 400 to 600 nm was recorded using a 360 nm excitation wavelength. Data were corrected for background scatter. Shifts in the center of the spectral mass were calculated as described (*17*). The resulting data were normalized and fit to a hyperbolic function using SigmaPlot (Jandel, Inc.) to obtain membrane partition coefficients.

(C) Fluorescence Resonance Energy Transfer. The self-association of synuclein was also monitored using fluorescence resonance energy transfer (FRET) by labeling one population of synuclein with an amine-reactive energy transfer donor, methoxy coumarin (Molecular Probes, Inc.), and labeling a second population with an amine-reactive energy transfer acceptor, dabcyl succinimydyl ester (Molecular Probes). Labeling was done by allowing a molar excess of probe to react with the protein at an elevated pH for 1 h at 4 °C. After dialysis to remove unreacted probe, labeling of the protein was confirmed by absorbance. The labeling stoichiometry, as estimated by absorption, was approximately 1 probe/protein. In the FRET assays, coumarin-synuclein was excited at 360 nm, and the decrease in its integrated emission intensity recorded from 380 to 460 nm was monitored as dabcyl-synuclein was added. In some experiments, lipid vesicles were present at all times whereas in other experiments no lipid vesicles were present.

Fluorescence Lifetime Measurements. Tyr fluorescence lifetimes of wild-type and A53T synuclein were measured at the National Synchrotron Light Source at Brookhaven National Laboratory (Upton, NY). Data were obtained from samples of aggregated and nonaggregated α-synuclein in the

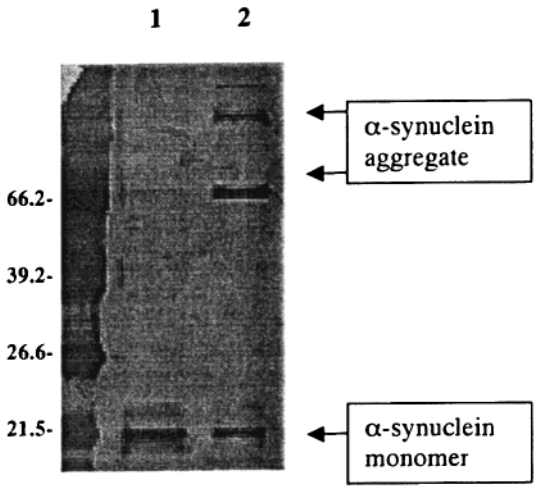

FIGURE 1: Silver-stained SDS−polyacrylamide gel showing purified monomeric α-synuclein in lane 1, and SDS-insoluble, irreversibly aggregated high molecular weight α-synuclein in lane 2. The mobility of low range molecular weight markers is shown on the left.

presence and the absence of membranes and at various pH conditions. Raw data were then analyzed to obtain the average lifetime (τ) of the fluorescent species in the various samples obtained.

Circular Dichroism Measurements. Circular dichroism spectra of A53T in 10 mM citrate/phosphate buffer, 7.5 mM NaCl were collected using an AVIV 62A DS circular dichroism spectrometer. Samples were contained in a cuvette of 0.1 cm path length. Molar ellipticities were calculated and plotted as described (*17*).

RESULTS

Characterization of α-Synuclein in Solution. Previous studies have found that synuclein purifies as an unstructured, random-coiled protein that changes from 3 ± 1% helix, 23 ± 8% β-sheet to 77 ± 3% helix, 1 ± 1% β-sheet when incubated with 20-fold excess of lipid by weight (*10, 13*). Using the same K2D algorithm as those authors (*18*), our purified protein gives a secondary structure of 9% helix, 35% β-sheet, and 56% random coil. We attribute the ability to purify synuclein in a more folded conformation (i.e., ~20% less random coil) as being due to the fact that our method does not involve either the ammonium sulfate precipitation step or boiling of supernatant used in previous purification protocols (*10, 16*). As shown in Figure 1, the purified protein behaves as a monomer on an SDS gel according to its electrophoretic mobility.

Binding of Synucleins to POPS and POPC Membranes. To better characterize the membrane binding properties of folded synuclein, we measured the partition coefficient of synuclein to large, unilamellar vesicles composed of lipids with electrically neutral, zwitterionic lipids (POPC) or to lipids with negatively charged headgroups (POPS). Experimental data were obtained either by monitoring the change in intrinsic fluorescence emanating from the four synuclein Tyr residues, or by doping the vesicles with a small amount of a detergent-like fluorescent probe, Laurdan (see Materials and Methods). In the case of the former, we followed binding by the shift in the tyrosine emission energy as it interacts with the highly charged membrane surface. In the latter case,

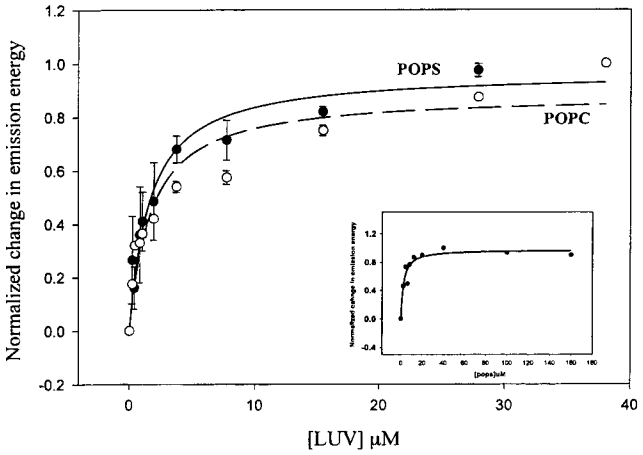

FIGURE 2: Binding of wild-type α-synuclein to 100% POPC and 100% POPS LUVs. The figure shows the fit of normalized data with a K_p of 1.6 ± 0.5 μM for POPC (○) and 1.6 ± 0.3 μM for POPS (●). Data were analyzed from shifts in the center of spectral mass of the intrinsic Tyr fluorescence from three independent experiments where the average shift corresponded to −450 cm^{-1} (−5.0 nm) for POPS and −450 cm^{-1} (−4.9 nm) for POPC. The graph in the inset shows data from an initial experiment where up to 160 μM lipid (POPS) was titrated into the protein solution.

Table 1: Comparison of Membrane Affinities of Synucleins

protein	binding to POPS (μM)	binding to POPC (μM)
α-synuclein wt	1.556 ± 0.32	1.645 ± 0.50
α (GRK2-phosphorylated)	0.913 ± 0.32	1.485 ± 0.50
α-synuclein (mutant A53T)	1.863 ± 0.27	0.690 ± 0.12

we followed binding by changes in the dielectric of the membrane surface as observed by the shift in the emission energy of the fluorescent probe, Laurdan, as the protein bound to the membrane surface. Membrane binding was monitored to lipid concentrations of 40 μM since in all cases complete saturation was reached at this value (see inset in Figure 2).

In contrast to previous studies that used prolonged incubation times and mechanical separation of products, and which found that α-synuclein only bound to small, unilamellar vesicles composed of specific phospholipids (*10, 16*), our equilibrium measurements show that α-synuclein binds with similar affinities to zwitterionic POPC and anionic POPS membranes immediately following addition of lipid (i.e., t < 1 min) (Figure 2). Moreover, the binding of α-synuclein to these large, unilamellar vesicles is quite strong as seen from the K_p values determined using Tyr or Laurdan fluorescence (Figure 2 and Table 1). These affinities are approximately a factor of 5−20 times stronger than those of classic membrane binding proteins (e.g., *17*).

We measured the membrane affinity of the point mutant A53T, which is involved in a small percentage of cases of Parkinson's disease (*3, 4*). This mutant also bound strongly to both types of lipid vesicles with affinities within error of the wild type (Figure 3 and Table 1). Interestingly, the affinity for membranes composed of electrically neutral POPC lipids was stronger than the affinity of the wild-type protein for these vesicles and was also stronger than its affinity for POPS membranes. We note that preliminary studies of β-synuclein, which binds to membranes with comparable affinities as the α form, indicate that it binds to POPS with a slightly higher affinity than to POPC.

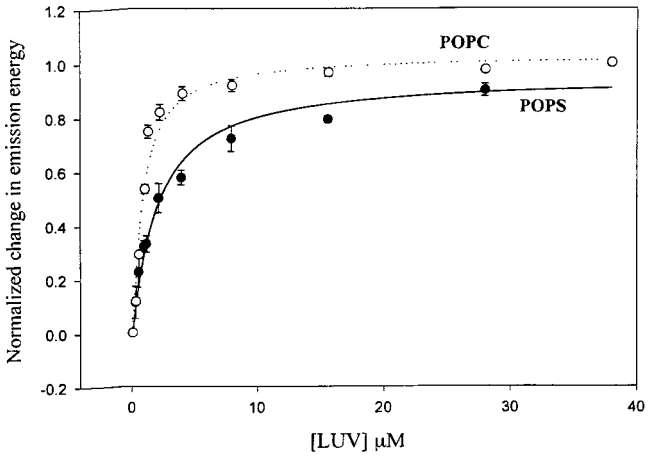

FIGURE 3: Binding of A53T α-synuclein to 100% POPC and 100% POPS LUVs. The figure shows the fit of normalized data with a K_p of 0.7 ± 0.1 μM for POPC (○) and 1.9 ± 0.3 μM for POPS (●). Data were analyzed from shifts in the center of spectral mass of the intrinsic Tyr fluorescence from three to six trials, which averaged −650 cm^{-1} (−6.5 nm) for POPS and −900 cm^{-1} (−10.7 nm) for POPC.

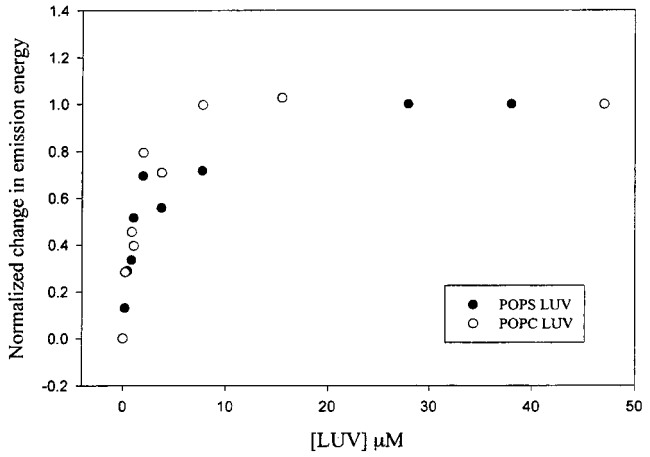

FIGURE 4: Binding of GRK2-phosphorylated α-synuclein to 100% POPC and 100% POPS LUVs. The figure shows typical data from one sample experiment using Laurdan-labeled vesicles to monitor binding. Normalized data from both Tyr fluorescence experiments and Laurdan experiments were fit with a K_p of 1.5 ± 0.5 μM for POPC (○) and 0.91 ± 0.3 μM for POPS (●). Data were analyzed from shifts in the center of spectral mass of the intrinsic Tyr fluorescence, which averaged −450 cm^{-1} (5.0 nm) for both POPS and POPC, or Laurdan fluorescence, which averaged −252 cm^{-1} (−4.5 nm) for POPS and −50 cm^{-1} (−1.2 nm) for POPC from two trials.

Effect of Phosphorylation of α-Synuclein on Lipid Binding. Recent evidence also shows that synuclein can be phosphorylated by G protein coupled receptor tyrosine kinases (*12*). It is possible that phosphorylation may alter its membrane binding affinity. We measured the membrane affinity of α-synuclein phosphorylated by GRK2 where the phosphorylation site is believed to be on Ser129 in the acidic C-terminal domain of the protein. Since phosphorylation can quench Tyr fluorescence, we monitored binding by the shift in the center of spectral mass of Laurdan-labeled lipids. Figure 4 shows a sample plot of the binding data. We find that the binding affinity of phosphorylated α-synuclein to POPS or POPC vesicles is similar and comparable to those observed with nonphosphorylated α-synuclein (Table 1).

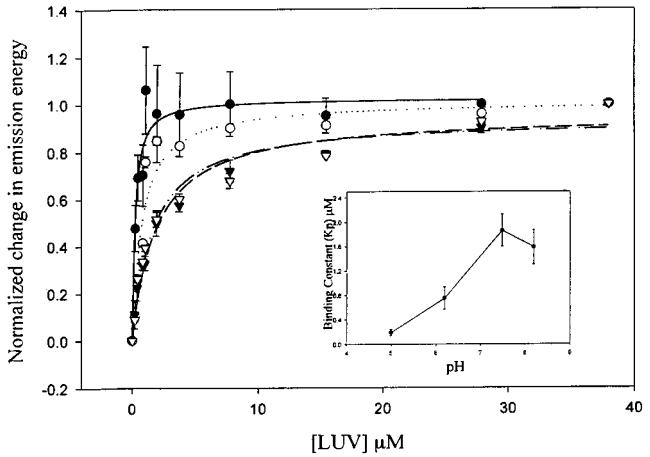

FIGURE 5: Effect of pH on the binding of A53T α-synuclein to 100% POPS LUVs. The figure shows the fits of normalized data with a K_p of 0.20 ± 0.05 μM at pH 5.0 (●), 0.75 ± 0.18 μM at pH 6.2 (○), 1.86 ± 0.26 μM at pH 7.5 (▼), and 1.59 ± 0.28 μM at pH 8.2 (▽). Data were analyzed from shifts in the center of spectral mass of the intrinsic Tyr fluorescence from three to six trials. The graph in the inset is a plot of the partition coefficients at the various pH points. Experiments at pH 5.0 and 6.2 were done using phosphate/citrate buffer with 150 mM sodium chloride, while those at pH 7.5 and 8.2 were done using Hepes buffer with 150 mM sodium chloride. The shifts in the center of mass corresponded to −620 cm^{-1} (−7.0 nm) at pH 5.0, −880 cm^{-1} (−9.9 nm) at pH 6.2, and −690 cm^{-1} (−7.7 nm) at pH 8.2.

Effect of pH on Membrane Binding. The C-terminus of synuclein is rich in acidic residues. We tested the idea that the acidic C-terminus of synuclein may weaken the binding of α-synuclein to negatively charged membrane surfaces due to charge repulsion. These studies were carried out by changing the buffer pH in a range which would cause the acidic residues in the protein to become more or less protonated, thereby effectively decreasing or increasing the acidity of the C-terminus. We used the mutant protein A53T in these experiments since we established that the mutant bound to the POPS LUVs with similar affinity as the wild-type protein and the mutation was not in the C-terminal domain.

We measured the binding affinity of A53T α-synuclein at four different pH points using a citrate/phosphate NaCl buffer for pH 5.0 and 6.2 and a Hepes/NaCl buffer for pH 7.5 and 8.2. We note that the membrane surface charge does not vary in this pH range (*19*). At pH 5.0, some of the acidic residues are expected to have some degree of protonation since the pK_a's of Asp and Glu should be shifted to higher pHs due to the anionic environment. Thus, at pH 5.0, we expect the protein to be less charged than at pH 7.5. This change in synuclein protonation clearly affects the binding affinity of A53T for POPS LUVs, which was 10-fold higher than that observed at pH 7.5. As the pH was increased from 5.0 to 8.2, the binding affinity decreased, as can be seen by the increasing value of the K_p (Figure 5). These data are consistent with the idea that charge repulsion from the C-terminus may contribute to the binding of synucleins to anionic surfaces.

Effect of Membranes on Secondary Structure. Previous membrane binding studies, that utilized prolonged membrane incubation, found that the membrane acts as a template to allow synuclein to fold into a helical conformation (*10*, *16*). However, since we monitored binding in real time im-

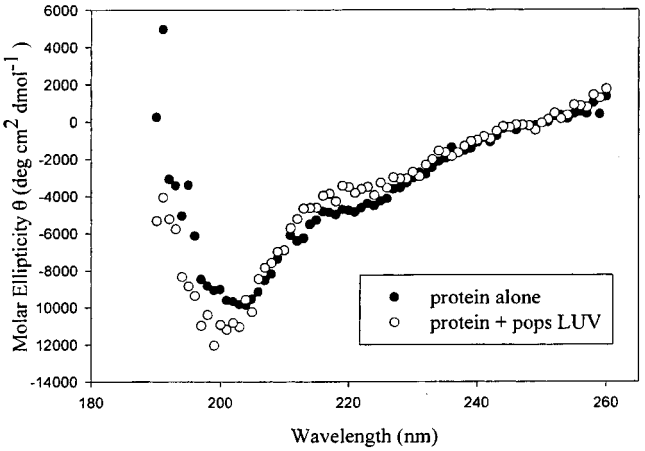

FIGURE 6: Circular dichroism spectra of 6.1 μM mutant A53T α-synuclein in the presence (65 μM) (○) and the absence (●) of 100% POPS LUVs in 5 mM citrate/10 mM phosphate buffer with 7.5 mM sodium chloride at pH 7.0 and 25 °C. Plotted spectra are the average of three measurements after the subtraction of vesicles or buffer background accordingly.

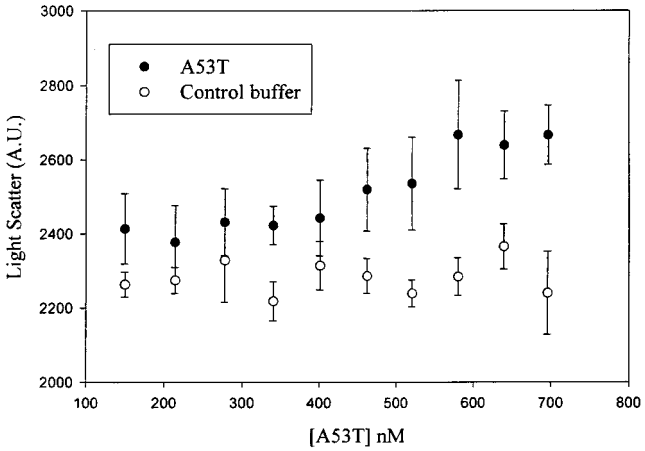

FIGURE 7: Light scatter measurements of mutant α-synuclein (A53T) by exciting at 350 nm and monitoring emission at 350 nm. The starting concentration of protein was 150 nM, and increasing amounts of protein were titrated into the initial solution. Data represent the average of three trials. Closed circles show data from addition of more protein, and open circles show control data from addition of an equivalent volume of buffer.

mediately after the addition of lipid to protein, it is uncertain whether membrane binding would alter its secondary structure. For reasons of availability, we tested this idea with the A53T mutant and note that this protein is reported to have an identical CD spectrum as wild type (*16*). The circular dichroism measurements were done under conditions of reduced salt (7.5 mM) at pH 7.0 using 10 mM phosphate/5 mM citrate buffer, and spectra were taken immediately following the addition of membranes. The plot of the relative molar ellipticities of the protein in the presence and absence of lipids is shown in Figure 6. The data indicate that the structure of A53T only results in a small increase (6%) in the overall (i.e., $\alpha + \beta$) secondary structure by the addition of lipids.

Detection of Early Synuclein Aggregate. While synuclein purifies as a monomer as indicated by electrophoretic mobility, over time it tends to aggregate. This time-dependent, SDS-resistant aggregation has been postulated to reflect the formation of fibrils in Parkinson's disease. We therefore attempted to characterize the aggregation of synuclein using fluorescence methods.

Interestingly, we found that all the synucleins tested had unusual fluorescence properties. Of the four Tyr residues, one is in the relatively hydrophobic N-terminus, and most likely contributes to the changes in fluorescence observed upon lipid binding. The other three are in the acidic C-terminus. While the typical emission maximum of Tyr is close to 305 nm, synuclein emission is centered at 350 nm even though no absorption was detectable above 285 nm, consistent with Tyr and not Trp residues. Moreoever, the excitation spectra were also red-shifted as compared to tyrosine.

Although there is a possibility that a Trp-containing contaminant that is not detectable by absorption is responsible for dominating the excitation and emission intensity of the four synuclein Tyr residues, which are present in large excess, it is also possible that these shifts are due to interactions of the phenol groups of the tyrosine residues in the excited state. These shifts in tyrosine emission due to excited state interactions have been previously characterized (*20*−*22*). If the phenol groups of the tyrosines are hydrogen bonded to proton acceptors (i.e., nearby acidic residues) in the ground state spectrum, emission from the phenolate ion would be facilitated. The phenolate emission energy is similar to Trp side chains. To determine whether this could be the case, we monitored the pH dependence of the emission of the electrophoretically monomeric form of α-synuclein. Starting at pH 5, we find that as the pH of the buffer increases, the average half-life of the excited species decreases from 3.7 ns at pH 4 to 3.03 ns at pH 7.4, which is consistent with an increased ionization of acidic residues that promotes thermal pathways of deactivation. This change in pH also resulted in a shift in the fluorescence emission to lower energy, presumably due to a stabilization of the interaction between acidic residues and Tyr side chains.

To determine whether the Tyr side chain of one synuclein molecule interacts with an acidic group on a neighboring synuclein, we monitored the changes in intrinsic fluorescence as increasing amounts of protein were added to a protein solution at an initial concentration of 150 nM. We find that the addition of protein causes a substantial reduction in emission energy (Figure 8, closed circles), indicating that protein association is occurring.

Self-association of α-synuclein with increased concentration was corroborated by fluorescence resonance energy transfer studies. In these experiments, we started with 150 nM coumarin-labeled synuclein and followed the loss in donor emission intensity as synuclein labeled with the nonfluorescent energy transfer acceptor dabcyl was added (Figure 9, closed circles). We find a linear decrease in donor fluorescence relative to controls using unlabeled protein, which clearly indicates protein association.

We used single-angle light scattering to detect whether the self-association of synuclein manifests as a change in particle size. We find that from 150 to 400 nM, the light scattering is constant. However, above 400 nM, the light scattering intensity begins to significantly rise up to and including the last point taken, 700 nM (Figure 7). Thus, these results coupled with the fluorescence studies indicate that from 150 to 400 nM, synuclein is forming small, reversible, prefibrillar oligomers.

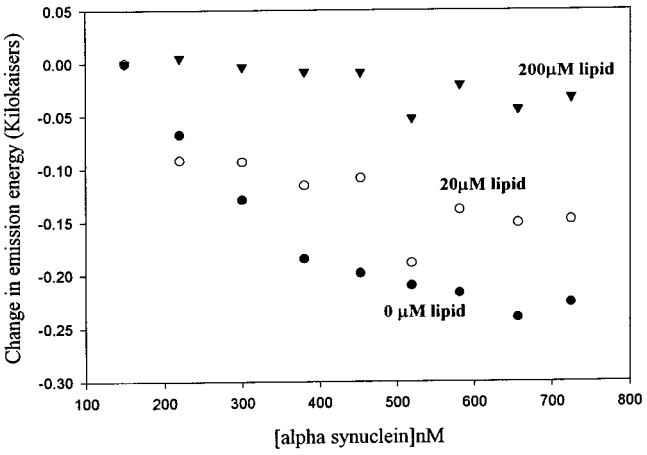

FIGURE 8: Effect of membranes on the self-association of wild-type α-synuclein. Increasing amounts of α-synuclein were titrated into 150 nM α-synuclein with 0 μM POPS LUV (●), 20 μM POPS LUV (○), or 200 μM POPS LUV (▼). Changes in the emission energy were calculated from measurements of the shifts in center of spectral mass of the intrinsic Tyr fluorescence and were −109 cm^{-1}(−1.28 nm) at 20 μM lipid, 24 cm^{-1} (−0.28 nm) at 200 μM lipid, and 224 cm^{-1} (−2.6 nm) in buffer. Data shown represent sample data from one experiment after subtraction of vesicle/buffer background.

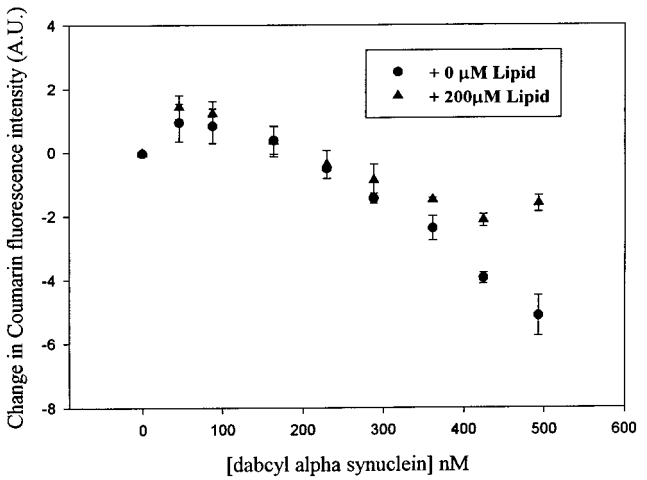

FIGURE 9: Fluorescence resonance energy transfer (FRET) assay between coumarin-labeled donor α-synuclein and dabcyl-labeled acceptor α-synuclein in the presence (▲) and in the absence (●) of 200 μM POPS LUVs. Data shown represent the change in integrated fluorescence emission intensity of coumarin-labeled α-synuclein, measured between 380 and 440 nm. The initial concentration was 75 nM labeled protein. Data have been corrected for vesicle background.

We also characterized the fluorescence properties of the SDS-resistant irreversibly aggregated synuclein shown in Figure 1. These aggregates formed during purification or during storage at 4 °C, and their formation was monitored by SDS-gel electrophoresis. We find that even though we could follow reversible synuclein association by shifts in the emission energy, the emission energy of the SDS-resistant aggregate was the same as the monomeric form. However, we found that the α-synuclein sample whose electrophoretic mobility corresponds to a monomer had a half-life of 3.03 ns, while the aggregated α-synuclein had a half-life of 2.0 ns, indicating that the aggregated state is characterized by a destabilization of the tyrosine excited state. These results correspond to previous findings that the conformational states of synuclein in the pre-fibril and fibril states differ (*23*). We note that recent studies have found intermolecular di-tyrosine cross-links in α-synuclein aggregates (*24*) which most likely contribute to these observed changes in fluorescence properties.

Role of Membranes in Synuclein Aggregation. To determine whether membrane binding serves as a template for α-synuclein aggregation and subsequent fibril formation, we monitored protein aggregation in the presence of membranes. In one series of studies, we determined whether the presence of membranes affected the shift in the emission energy with increasing amounts of protein. Unlabeled α-synuclein was titrated into a dilute (150 nM) solution of α-synuclein at pH 7.4 as described above. As the concentration of the protein increased, there was an increased red shift in the center of spectral mass consistent with protein association. To determine whether the presence of membranes affects association, we repeated this experiment in the presence of 20 and 200 μM POPS. We found that protein association was severely inhibited by the presence of lipid membranes as shown in Figure 8, even though membrane binding increases the effective concentration by a factor of 100 (*25*).[1] Thus, either the protein association sites in synuclein are occluded when the protein binds to the membrane, or membrane binding alters the tertiary conformation of synuclein such that oligomerization is inhibited.

The effect of membranes on synuclein self-association was also monitored by fluorescence resonance energy transfer as described above. In Figure 9, we present data showing that in the presence of lipid, energy transfer is inhibited until concentrations where membrane crowding is expected to occur, further supporting the idea that membrane binding inhibits the oligomerization of synuclein.

DISCUSSION

Although the function of synuclein is unknown, there is evidence that it is involved in the trafficking of synaptic vesicles. The potential role in trafficking implies that these proteins associate to lipid membranes. Previous workers have studied the association of synuclein to membranes (*10*, *16*, *26*). These studies found a clear preference of synuclein to highly curved, negatively charged lipid vesicles. These studies all incubated the protein for an extended period before mechanically separating bound and unbound lipid. In our assays, we viewed association immediately following the addition of lipid to protein. Using this real time equilibrium method, we find that synuclein binds strongly to the relatively flat surfaces of large, unilamellar vesicles even when the electrical charge of the surface is neutral. This initial binding does not induce changes in the secondary structure of the protein. Unfortunately, our attempts at extending the incubation time result in vesicle fusion of POPS which is promoted with increased vesicle curvature. These observations point to a scenario in which synuclein binds to lipids in its native, nonhelical form but over time helices form possibly through penetration into the lipid matrix, self-association, and/or vesicle fusion where they become kinetically trapped on the membrane and are unable to dissociate upon mechanical

[1] Note that we always observed a slight blue shift in Tyr fluorescence as more lipid was titrated into a given concentration of protein, possibly representing a breaking up in the association of the protein.

separation. Mechanistically, the highly curved anionic lipids used in previous studies might chaperone synuclein structure because charge repulsion by the anionic C-terminal tail of synuclein may help to correctly orient the protein on negatively charged lipids, promoting the formation of the helical structure. Positive residues in the N-terminus would be expected to either initiate or promote these changes. This orienting effect due to charge would not be promoted on neutral membranes or on flat membrane surfaces that require proteins to have a higher affinity to bind as compared to highly curved surfaces. Support for the role of the C-terminus in membrane binding comes from studies where we show that lowering the pH of the folded protein, which reduces the negative charge of the protein, greatly increases the binding constant without altering the secondary structure. We note that our fluorescence assays only monitor the binding population, and it is possible that a portion of the proteins are not associating with membranes. A small lipid binding population may be the reason that binding to zwitterionic membrane surfaces and large vesicles was not seen by methods that physically separated the proteoliposomes from pure lipids. However, the extent of the observed changes in fluorescence parameters coupled with energy transfer results indicates that a substantial population of the proteins bind to membranes. Thus, it is likely that the lack of binding to LUVs and POPC vesicles previously observed resulted from a shift in the binding equilibria during separation, and/or a possible change in the POPS proteoliposome structure due to fusion. As mentioned, events that may accompany the transition to a helical state of the protein, such as aggregation or lipid penetration, could kinetically trap synuclein on the membrane.

By following the fluorescence from lipid and protein in different assays, we confirmed that the binding of α-synucleins to membranes is very strong and nonspecific with respect to surface charge. Interaction of synuclein with POPC lipids may occur through the hydrophobic domain of the protein (see *15*), and membrane interaction through this region would then account for inhibition of synuclein self-association (see below). The pH dependence of these affinities indicates that repulsive forces, presumably in the acidic C-terminus, weaken binding to anionic lipids. Interestingly, the A53T mutant and β-synuclein appear to have some charge specificity. The β protein, which differs from the α protein by the deletion of a central domain, shows enhanced binding for POPS. This enhancement may be caused by reduced repulsion from the C-terminus due to differing orientation with respect to the lipid binding domain. Alternately, the A53T mutant shows enhanced binding to POPC which may be the result of subtle differences in the orientation of this protein on the membrane surface, or to protein−protein interactions on the membrane surface which decrease the off rate.

Plasma membranes contain ∼30% anionic lipids, and it is unclear whether the somewhat minor differences in affinity of these synucleins would affect their membrane association in vivo. Further, there is increasing evidence that lipids in membranes may not be homogeneously distributed but localized in domains which would serve to increase differences in affinity between wild-type and A53T mutant α-synuclein. Under conditions where synuclein must compete with other proteins for available lipid and/or for as of yet unknown protein partners, these small differences may play a role.

Perhaps the most significant finding of this study is that membrane binding serves to reduce the early oligomerization or premature protein−protein association of synuclein. This inhibition of oligomerization is not expected since membrane binding should concentrate the protein on the surface and promote protein−protein association. Our results suggest that the protein−protein interaction site is at least partially occluded upon membrane binding and point to the hydrophobic domain as being the interaction region. The protein−protein association we observe in solution was done under short-term, dilute conditions that should precede nucleation. With increasing monomer concentrations, this association will eventually result in prefibrillar oligomers (*13*) which ultimately undergo a drastic change in secondary structure to form insoluble fibrillar aggregates. Therefore, in order for synuclein aggregation to occur, the apparently weaker protein association must compete with strong lipid binding. While this does not appear to be the case for phosphorylated synuclein, other modifications such as nitration may allow for competitive interactions. Also, other interactive proteins, such as synphilin (*27*), may play a role. Thus, under conditions where membrane binding is inhibited or protein association is enhanced, oligomerization and fibril formation may occur.

ACKNOWLEDGMENT

We are grateful to Drs. John Sutherland and John Trunk at Brookhaven National Laboratories for their help with the time-resolved measurements, and to Dr. Daniel Raleigh and Mr. Satoshi Sato for their help with the CD measurements, to Dr. Andrew Morris for providing us with some of the purified proteins used here and with the α-synuclein and A53T α-synuclein bacterial lines, and to an anonymous reviewer for helpful comments.

REFERENCES

1. Galvin, J. E., Giasson, B., Hurtig, H. I., Lee, V. M., and Trojanowski, J. Q. (2000) *Am. J. Pathol. 157*, 361−368.
2. Duda, J. E., Lee, V. M., and Trojanowski, J. Q. (2000) *J. Neurosci. Res. 61*, 121−127.
3. Polymeropoulos, M. H., Lavedan, C., Leroy, E., Ide, S., Dehejia, A., Dutra, A., Pike, B., Root, H., Rubenstein, J., Boyer, R., Sternoos, E., Chanraseskhara, S., Athanassiadou, A., Papapetropoulos, T., Johnson, W. G., Lazzarini, A., Di Iorio, G., Golbe, L., and Nussbaum, R. L. (1997) *Science 276*, 2045−2047.
4. Kruger, R., Muller, T., and Riess, O. (2000) *J. Neural Transm. 107*, 31−40.
5. Bruening, W., Giasson, B. I., Klein-Szanto, A. J., Lee, V. M., Trojanowski, J. Q., and Godwin, A. K. (2000) *Cancer 88*, 2154−2163.
6. Hashimoto, M., Hsu, L. J., Xia, Y., Takeda, A., Sisk, A., Sundsmo, M., and Masliah, E. (1999) *Neuroreport 10*, 717−721.
7. Giasson, B. I., Duda, J. E., Murray, I. V., Chen, Q., Souza, J. M., Hurtig, H. I., Ischiropoulos, H., Trojanowski, J. Q., and Lee, V. M. (2000) *Science 290*, 985−989.
8. Clayton, D. F., and George, J. M. (1998) *Trends Neurosci. 21*, 249−254.
9. Jenco, J. M., Rawlingson, A., Daniels, B., and Morris, A. J. (1998) *Biochemistry 37*, 4901−4909.
10. Davidson, W. S., Jonas, A., Clayton, D. F., and George, J. M. (1998) *J. Biol. Chem. 273*, 9443−9449.

11. Ellis, C. E., Schwartzberg, P. L., Grider, T. L., Fink, D. W., and Nussbaum, R. L. (2000) *J. Biol. Chem.*
12. Pronin, A. N., Morris, A. J., Surguchov, A., and Benovic, J. L. (2000) *J. Biol. Chem. 275*, 26515−26522.
13. Conway, K. A., Lee, S. J., Rochet, J. C., Ding, T. T., Williamson, R. E., and Lansbury, P. T., Jr. (2000) *Proc. Natl. Acad. Sci. U.S.A. 97*, 571−576.
14. Wood, S. J., Wypych, J., Steavenson, S., Louis, J. C., Citron, M., and Biere, A. L. (1999) *J. Biol. Chem. 274*, 19509−19512.
15. Giasson, B. I., Murray, I. V., Trojanowski, J. Q., and Lee, V. M. (2000) *J. Biol. Chem.*
16. Jo, E., McLaurin, J., Yip, C. M., St. George-Hyslop, P., and Fraser, P. E. (2000) *J. Biol. Chem. 275*, 34328−34334.
17. Wang, T., Pentyala, S., Rebecchi, M. J., and Scarlata, S. (1999) *Biochemistry 38*, 1517−1524.
18. Andrade, M. A., Chacon, P., Merelo, J. J., and Moran, F. (1993) *Protein Eng. 6*, 383−390.
19. Scarlata, S., and Rosenberg, M. (1990) *Biochemistry 29*, 10233−10240.
20. Dietze, E. C., Wang, R. W., Lu, A. Y. H., and Atkins, W. M. (1996) *Biochemistry 35*, 6745−6753.
21. Narayanaswami, V., Frolov, A., Schroder, F., Oikawa, K., Kay, C. M., and Ryan, R. O. (1996) *Arch. Biochem. Biophys. 334*, 143−150.
22. Turner, R. J., and Moore, G. J. (1992) *Biochim. Biophys. Acta 1117*, 265−270.
23. El-Agnaf, O. M., and Irvine, G. B. (2000) *J. Struct. Biol. 130*, 300−309.
24. Souza, J. M., Giasson, B. I., Chen, Q., Lee, V. M., and Ischiropoulos, H. (2000) *J. Biol. Chem. 275*, 18344−18349.
25. Runnels, L., and Scarlata, S. (1999) *Biochemistry 38*, 1488−1496.
26. Perrin, R. J., Woods, W. S., Clayton, D. F., and George, J. M. (2000) *J. Biol. Chem. 275*, 34393−34398.
27. Engelender, S., Kaminsky, Z., Guo, X., Sharp, A. H., Amaravi, R. K., Kleiderlein, J. J., Margolis, R. L., Troncoso, J. C., Lanahan, A. A., Worley, P. F., Dawson, V. L., Dawson, T. M., and Ross, C. A. (1999) *Nat. Genet. 22*, 110−114.

BI002952N